
01 Feb 2002

A Mössbauer Spectral Study of the Magnetic Properties of $\text{Ho}_2\text{Fe}_{17}$ and $\text{Ho}_2\text{Fe}_{17}\text{D}_{3.8}$

Gary J. Long

Missouri University of Science and Technology, glong@mst.edu

Olivier Isnard

Fernande Grandjean

Missouri University of Science and Technology, grandjeanf@mst.edu

Follow this and additional works at: https://scholarsmine.mst.edu/chem_facwork

 Part of the [Chemistry Commons](#)

Recommended Citation

G. J. Long et al., "A Mössbauer Spectral Study of the Magnetic Properties of $\text{Ho}_2\text{Fe}_{17}$ and $\text{Ho}_2\text{Fe}_{17}\text{D}_{3.8}$," *Journal of Applied Physics*, vol. 91, no. 3, pp. 1423-1430, American Institute of Physics (AIP), Feb 2002. The definitive version is available at <https://doi.org/10.1063/1.1428794>

This Article - Journal is brought to you for free and open access by Scholars' Mine. It has been accepted for inclusion in Chemistry Faculty Research & Creative Works by an authorized administrator of Scholars' Mine. This work is protected by U. S. Copyright Law. Unauthorized use including reproduction for redistribution requires the permission of the copyright holder. For more information, please contact scholarsmine@mst.edu.

A Mössbauer spectral study of the magnetic properties of $\text{Ho}_2\text{Fe}_{17}$ and $\text{Ho}_2\text{Fe}_{17}\text{D}_{3.8}$

Gary J. Long^{a)}

Department of Chemistry, University of Missouri-Rolla, Rolla, Missouri 65409-0010

Olivier Isnard^{b)}

Laboratoire de Cristallographie du CNRS, associé à l'Université J. Fourier et à l'INPG, CNRS, F-38042 Grenoble, France

Fernande Grandjean^{c)}

Institut de Physique, B5, Université de Liège, B-4000 Sart-Tilman, Belgium

(Received 17 September 2001; accepted for publication 27 October 2001)

The Mössbauer spectra of $\text{Ho}_2\text{Fe}_{17}$ and $\text{Ho}_2\text{Fe}_{17}\text{D}_{3.8}$ have been measured between 4.2 and 295 K and analyzed with a model which takes into account both the disordered nonstoichiometric hexagonal $\text{Th}_2\text{Ni}_{17}$ -like structure and the basal orientation of the iron magnetic moments. The isomer shifts of the five crystallographically inequivalent iron sites in both $\text{Ho}_2\text{Fe}_{17}$ and $\text{Ho}_2\text{Fe}_{17}\text{D}_{3.8}$ follow the sequence of Wigner-Seitz cell volumes and their temperature dependence follows the typical second-order Doppler shift. An increase in the weighted average isomer shift upon deuterium insertion results from the lattice expansion. The sequence of the site-averaged hyperfine fields is in agreement with the increasing number of iron near neighbors. The five quadrupole interactions agree with those observed in the paramagnetic spectra of other $R_2\text{Fe}_{17}$ compounds. For the dumbbell $4e$ and $4f$ sites, the asymmetry parameter and the θ angle are zero and 90° in agreement with the site point symmetry and the basal orientation of the iron magnetic moment. For the $6g$ site, the asymmetry parameter is zero in agreement with the site point symmetry. In both compounds the $12j$ site asymmetry parameter is 0.9 and for the $12k$ site this parameter increases from 0.0 in $\text{Ho}_2\text{Fe}_{17}$ to 0.8 in $\text{Ho}_2\text{Fe}_{17}\text{D}_{3.8}$ as a result of the insertion of an additional deuterium near neighbor. The θ angles for the magnetically inequivalent $12j$ and $12k$ sites differ by 60° as expected in the hexagonal symmetry. The variations with rare-earth of the weighted average isomer shifts and hyperfine fields in $R_2\text{Fe}_{17}$, $R_2\text{Fe}_{17}\text{H}_x$, and $R_2\text{Fe}_{17}\text{N}_3$, are discussed in terms of the lanthanide contraction and lattice expansion upon insertion of hydrogen, or deuterium, or nitrogen and the axial and basal magnetic anisotropy. © 2002 American Institute of Physics. [DOI: 10.1063/1.1428794]

I. INTRODUCTION

The rare-earth iron intermetallic compounds, $R_2\text{Fe}_{17}$, possess a wide variety of physical properties because it is possible to both vary the rare-earth and to insert interstitial atoms, such as hydrogen, deuterium, carbon, and nitrogen, into the $R_2\text{Fe}_{17}$ lattice. The result of both of these variations is to provide a wide range of magnetic interactions in $R_2\text{Fe}_{17}$, interactions which we have been studying extensively by different techniques, i.e., neutron diffraction, magnetic measurements, and Mössbauer spectroscopy.

The variation of the rare-earth size leads to two different crystallographic structures. With the lighter but larger rare-earth atoms from Ce to Gd the ordered, stoichiometric, rhombohedral $\text{Th}_2\text{Zn}_{17}$ -like structure forms. In contrast, with the heavier but smaller rare-earth atoms from Gd to Lu the often disordered, and/or nonstoichiometric, hexagonal $\text{Th}_2\text{Ni}_{17}$ -like structure forms. Further, the homogeneity range, x , of the $R_2\text{Fe}_{17\pm x}$ compounds, where R is a heavy

rare earth, broadens¹⁻⁴ with increasing rare-earth atomic number.

The insertion of deuterium into $\text{Ho}_2\text{Fe}_{17}$ to form $\text{Ho}_2\text{Fe}_{17}\text{D}_{3.8}$ offers, over the insertion of hydrogen, the advantage both of making the gravimetric analysis of the deuterium content more accurate and of reducing the incoherent neutron scattering. The thermodynamics of the insertion of hydrogen or deuterium into the $\text{Ho}_2\text{Fe}_{17}$ structure has been reported^{5,6} and the isotherms recorded for $\text{Ho}_2\text{Fe}_{17}$ are typical of a solid solution at room temperature. The maximum number of deuterium atoms that can be inserted into $\text{Ho}_2\text{Fe}_{17}$ is 3.8 per formula unit, a number which is smaller than the five deuterium atoms that can be inserted into the light rare-earth $R_2\text{Fe}_{17}$ compounds.

An earlier neutron diffraction study⁴ of $\text{Ho}_2\text{Fe}_{17}$ and its deuteride indicated actual stoichiometries of $\text{Ho}_2\text{Fe}_{17.67}$ and $\text{Ho}_2\text{Fe}_{17.67}\text{D}_{3.8}$, however, for the sake of simplicity, we will refer herein to these compounds as $\text{Ho}_2\text{Fe}_{17}$ and $\text{Ho}_2\text{Fe}_{17}\text{D}_{3.8}$. This study⁴ also confirmed that both compounds crystallize with the disordered hexagonal $\text{Th}_2\text{Ni}_{17}$ -like structure and indicated that the lattice expands anisotropically upon deuterium insertion with relative expansions of 1.46% and 0.68% along the a and c axes, respec-

^{a)}Electronic mail: glong@umr.edu

^{b)}Electronic mail: isnard@labs.polycnrs-ge.fr

^{c)}Electronic mail: fgrandjean@ulg.ac.be

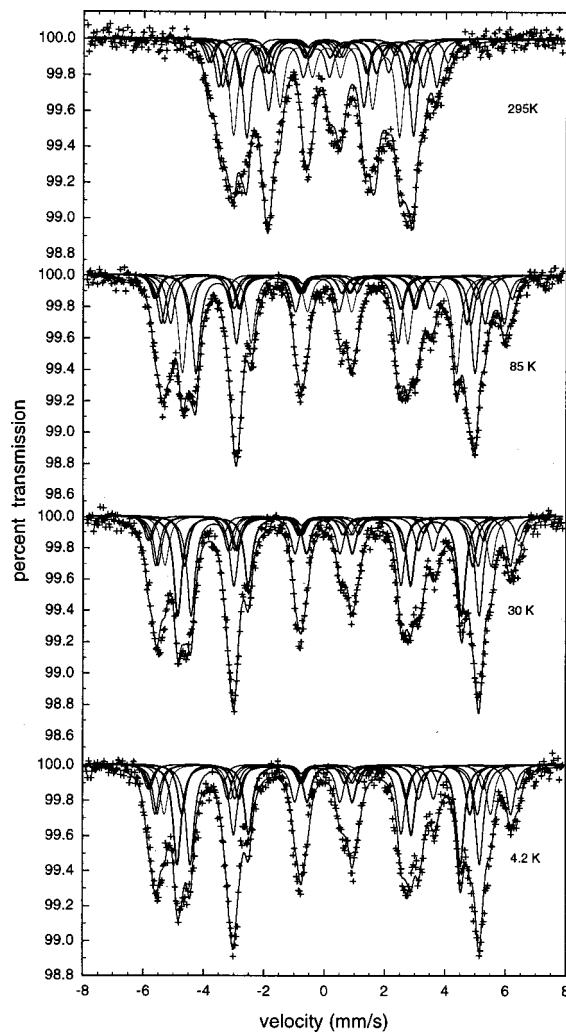


FIG. 1. The Mössbauer spectra of $\text{Ho}_2\text{Fe}_{17}$ obtained at the indicated temperatures.

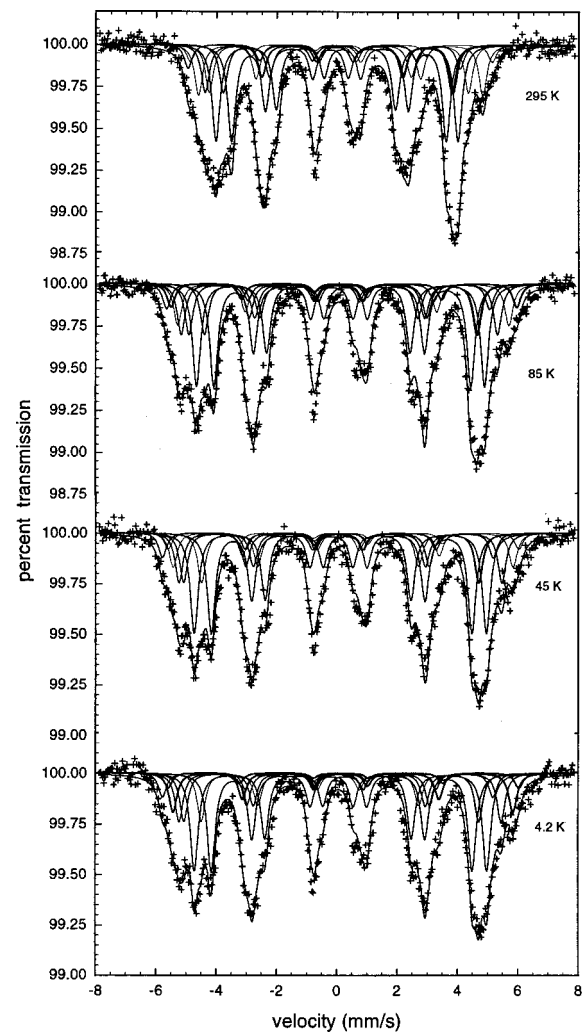


FIG. 2. The Mössbauer spectra of $\text{Ho}_2\text{Fe}_{17}\text{D}_{3.8}$ obtained at the indicated temperatures.

tively. The deuterium atoms are found to occupy interstitial sites in the vicinity of the holmium atoms, with a preference⁷ for the larger octahedral $6h$ sites, rather than the smaller tetrahedral $12i$ sites. In $\text{Ho}_2\text{Fe}_{17}\text{D}_{3.8}$, approximately three deuterium atoms per formula unit occupy the octahedral $6h$ sites and one deuterium atom occupies the tetrahedral $12i$ sites. The one-sixth partial occupancy of the $12i$ site has been discussed^{7,8} in terms of the Switendick–Westlake⁹ criteria.

The extreme sensitivity of the intradumbbell Fe–Fe exchange interactions to the Fe–Fe distance in $R_2\text{Fe}_{17}$ compounds has been extensively discussed by Givord and Lemaire^{2,10,11} in terms of the Néel–Slater curve. In an overly simplistic way, negative exchange interactions may be associated with the very short Fe–Fe distance within the dumbbell. Because of the lanthanide contraction, the unit cell parameters decrease with increasing rare-earth atomic number, and the Fe–Fe dumbbell distance decreases and becomes even more critical^{2,10} in determining the magnetic interactions in $\text{Lu}_2\text{Fe}_{17}$. The decrease in unit cell volume, which accompanies the lanthanide contraction, has two consequences for the hydrogen or deuterium containing materials. First, the number of hydrogen or deuterium atoms that can be

inserted into the lattice decreases because the volume of the tetrahedral interstitial $12i$ site decreases. Indeed, no hydrogen or deuterium can be inserted^{2,10} into the $12i$ site in $\text{Lu}_2\text{Fe}_{17}$. Second, the ordering temperatures of the heavier $R_2\text{Fe}_{17}$ compounds are more sensitive to hydrogen or deuterium insertion because their unit cell volume is smaller. Deuterium insertion into $\text{Ho}_2\text{Fe}_{17}$ induces a 165 K ordering temperature increase, from 335 to 500 K, an increase which is larger than observed^{8,12} for the lighter rare-earth compounds, $\text{Gd}_2\text{Fe}_{17}$, $\text{Tb}_2\text{Fe}_{17}$, or $\text{Dy}_2\text{Fe}_{17}$, but smaller than observed^{13,14} for the heavier rare-earth compounds, $\text{Er}_2\text{Fe}_{17}$, $\text{Tm}_2\text{Fe}_{17}$, or $\text{Lu}_2\text{Fe}_{17}$.

Both because holmium has a negative second-order Stevens coefficient, a coefficient which favors a basal magnetic anisotropy, and because iron is also known¹⁵ to favor a basal magnetic anisotropy in the $R_2\text{Fe}_{17}$ compounds, the iron and holmium moments in $\text{Ho}_2\text{Fe}_{17}$ are expected to lie in the basal plane. Indeed, neutron diffraction measurements^{3,4} have shown that the holmium and iron magnetic moments are antiferromagnetically aligned in the basal plane of both $\text{Ho}_2\text{Fe}_{17}$ and $\text{Ho}_2\text{Fe}_{17}\text{D}_{3.8}$.

In this paper, the temperature dependence of the Mössbauer spectra of $\text{Ho}_2\text{Fe}_{17}$ and $\text{Ho}_2\text{Fe}_{17}\text{D}_{3.8}$ is reported. This

TABLE I. Mössbauer spectral hyperfine parameters for $\text{Ho}_2\text{Fe}_{17}$.

	T, K	$4f$	$4e$	$6g_4$	$6g_2$	$12j_8$	$12j_4$	$12k_8$	$12k_4$	Wt. Ave.
H, kOe	4.2	365.6	380.0	326.5	340.5	297.7	333.9	289.8	295.5	317.3
	30	364.0	380.1	327.5	341.5	295.5	333.0	290.0	295.0	316.7
	85	352.0	367.1	313.5	328.5	286.0	321.0	280.0	283.0	305.4
	155	326.0	342.6	287.0	302.0	261.0	292.0	257.0	259.0	280.2
	225	290.2	311.7	247.8	259.6	228.0	257.0	226.0	229.0	246.3
	295	223.7	246.0	185.9	208.2	169.0	197.0	168.0	171.0	186.4
$\delta_i^a, \text{mm/s}$	4.2	0.250	0.260	-0.070	-0.070	0.065	0.065	0.005	0.005	0.054
	30	0.245	0.255	-0.070	-0.070	0.063	0.063	0.005	0.005	0.052
	85	0.225	0.240	-0.090	-0.090	0.055	0.055	-0.010	-0.010	0.038
	155	0.170	0.180	-0.130	-0.130	0.015	0.015	-0.040	-0.040	-0.001
	225	0.110	0.130	-0.175	-0.175	-0.028	-0.028	-0.085	-0.085	-0.047
	295	0.040	0.050	-0.205	-0.205	-0.070	-0.070	-0.130	-0.130	-0.094
$e^2Qq/2, \text{mm/s}$	-	-0.15	-0.15	-0.51	-0.51	0.60	0.60	-0.54	-0.54	-
η	-	0	0	0	0	0.9	0.9	0	0	-
θ, deg	4.2	90	90	30	25	0	62	30	90	-
	30	90	90	32	25	0	62	30	90	-
	85	90	90	32	25	4	64	30	90	-
	155	90	90	28	20	6	63	30	90	-
	225	90	90	26	18	10	65	30	90	-
	295	90	90	26	18	25	55	30	90	-
Area, %	4.2-295	11.1	5.55	11.1	5.55	22.2	11.1	22.2	11.1	-

^aThe isomer shifts are given relative to room temperature α -iron foil.

study completes our Mössbauer spectral investigation of the R_2Fe_{17} compounds and their hydrides or deuterides, and thus permits a comparative analysis of their hyperfine parameters and lattice properties as a function of the rare-earth atom.

II. EXPERIMENT

The samples studied herein are those described⁴ earlier. Mössbauer spectral absorbers of ca. 36 mg/cm² were pre-

TABLE II. Mössbauer spectral hyperfine parameters for $\text{Ho}_2\text{Fe}_{17}\text{D}_{3.8}$.

	T, K	$4f$	$4e$	$6g_4$	$6g_2$	$12j_8$	$12j_4$	$12k_8$	$12k_4$	Wt. Ave.
H, kOe	4.2	348.9	360.0	306.9	338.8	282.4	323.9	284.2	283.2	307.0
	45	349.0	360.0	307.0	339.0	282.0	325.0	284.0	282.7	306.9
	85	340.0	355.0	303.3	331.1	277.5	315.0	280.6	278.0	301.4
	155	329.0	352.0	294.0	318.1	266.4	301.0	271.7	265.6	290.7
	225	313.2	330.0	276.0	299.0	253.7	286.0	257.3	253.0	275.5
	295	292.0	310.0	253.0	279.0	232.0	264.0	235.0	233.0	253.7
$\delta_i^a, \text{mm/s}$	4.2	0.170	0.185	-0.085	-0.085	0.120	0.120	0.078	0.078	0.084
	45	0.170	0.180	-0.085	-0.085	0.110	0.110	0.075	0.075	0.079
	85	0.165	0.185	-0.085	-0.085	0.115	0.115	0.085	0.085	0.084
	155	0.135	0.160	-0.115	-0.115	0.080	0.080	0.055	0.055	0.052
	225	0.100	0.120	-0.165	-0.165	0.045	0.045	0.015	0.015	0.010
	295	0.070	0.090	-0.210	-0.210	0.010	0.010	-0.020	-0.020	-0.027
$e^2Qq/2, \text{mm/s}$	-	-0.15	-0.15	-0.52	-0.52	0.60	0.60	-0.55	-0.55	-
η	-	0	0	0	0	0.9	0.9	0.8	0.8	-
θ, deg	4.2	90	90	28	20	10	58	30	90	-
	45	90	90	28	20	10	55	30	90	-
	85	90	90	28	20	10	55	30	90	-
	155	90	90	40	25	25	70	30	90	-
	225	90	90	44	15	25	70	32	90	-
	295	90	90	46	15	25	65	32	90	-
Area, %	4.2	9.3	3.6	11.6	5.8	23.2	11.6	23.2	11.6	-
	45	8.1	3.9	11.7	5.9	23.5	11.7	23.5	11.7	-
	85	9.3	5.3	11.4	5.7	22.8	11.4	22.8	11.4	-
	155	12.0	4.8	11.1	5.5	22.2	11.1	22.2	11.1	-
	225	10.6	6.2	11.1	5.5	22.2	11.1	22.2	11.1	-
	295	11.8	4.1	11.2	5.6	22.4	11.2	22.4	11.2	-

^aThe isomer shifts are given relative to room temperature α -iron foil.

pared from powdered samples which had been sieved to a 0.045 mm or smaller diameter particle size. The Mössbauer spectra were obtained between 4.2 and 295 K on a constant-acceleration spectrometer which utilized a rhodium matrix cobalt-57 source and was calibrated at room temperature with α -iron foil. The studies were carried out in a Janis Supravertemp cryostat in which the samples were never exposed to a vacuum. The spectra have been fit as discussed below and the estimated relative errors are at most ± 1 kOe for the hyperfine fields, ± 0.005 mm/s for the isomer shifts, ± 0.01 mm/s for the quadrupole interactions, $\pm 1^\circ$ for the θ angles, ± 0.1 for the asymmetry parameter, and $\pm 0.5\%$ for the relative spectral component areas. The absolute errors are larger by a factor of approximately 2.

III. MÖSSBAUER SPECTRAL RESULTS

The Mössbauer spectra of $\text{Ho}_2\text{Fe}_{17}$ obtained at 4.2, 30, 85, and 295 K and of $\text{Ho}_2\text{Fe}_{17}\text{D}_{3.8}$ obtained at 4.2, 45, 85, and 295 K are shown in Figs. 1 and 2, respectively. Because, as is indicated by the neutron diffraction measurements on both compounds,⁴ the iron magnetic moments are oriented within the basal plane of the unit cell, the Mössbauer spectra have been analyzed^{12,13} with eight sextets assigned to the magnetically inequivalent 4e, 4f, 6g₄, 6g₂, 12j₈, 12j₄, 12k₈, and 12k₄ iron sites. A single linewidth of 0.32 mm/s has been used and the relative areas of the 6g₄, 6g₂, 12j₈, 12j₄, 12k₈, and 12k₄ sextets have been constrained in the ratio 4:2:8:4:8:4. The relative areas of the 4e and 4f sites have been adjusted. The isomer shifts, δ , and the quadrupole interactions, $e^2Qq/2$, of the crystallographically inequivalent sites, and the hyperfine fields, H , and angles, θ , between the principal axis of the electric field gradient axis and the hyperfine field, of the magnetically inequivalent sites have been adjusted. The θ angles for the 4e and 4f sites were fixed at 90° as expected if the iron magnetic moments and hyperfine fields are in the basal plane of the unit cell. The asymmetry parameter, η , for the 4e, 4f, and 6g sites was set equal to zero in agreement with the point symmetry of these sites. The asymmetry parameters for the 12j and 12k sites were adjusted and the best fits were obtained for η values of 0.9 and 0, for $\text{Ho}_2\text{Fe}_{17}$ and 0.9 and 0.8, for $\text{Ho}_2\text{Fe}_{17}\text{D}_{3.8}$. The resulting hyperfine parameters and relative areas for $\text{Ho}_2\text{Fe}_{17}$ and $\text{Ho}_2\text{Fe}_{17}\text{D}_{3.8}$ are given in Tables I and II, respectively.

On the basis of the disorder observed⁴ in $\text{Ho}_2\text{Fe}_{17}$, the expected relative areas of the 4e, 4f, 6g, 12j, and 12k spectral components are 2.84%, 9.79%, 17.47%, 34.95%, and 34.95%, respectively. Even though the relative areas given in Table I have been adjusted, they do not deviate substantially from the expected areas. The relative areas given in Table II for $\text{Ho}_2\text{Fe}_{17}\text{D}_{3.8}$ are similar to those observed for $\text{Ho}_2\text{Fe}_{17}$ and do not deviate substantially from the expected areas. Indeed, no significant variation is expected upon deuterium insertion into the interstitial sites in the absence of substantial modification of the crystal structure.

IV. DISCUSSION AND CONCLUSIONS

The temperature dependence of the isomer shift of the five different iron sites in $\text{Ho}_2\text{Fe}_{17}$ and $\text{Ho}_2\text{Fe}_{17}\text{D}_{3.8}$ is shown

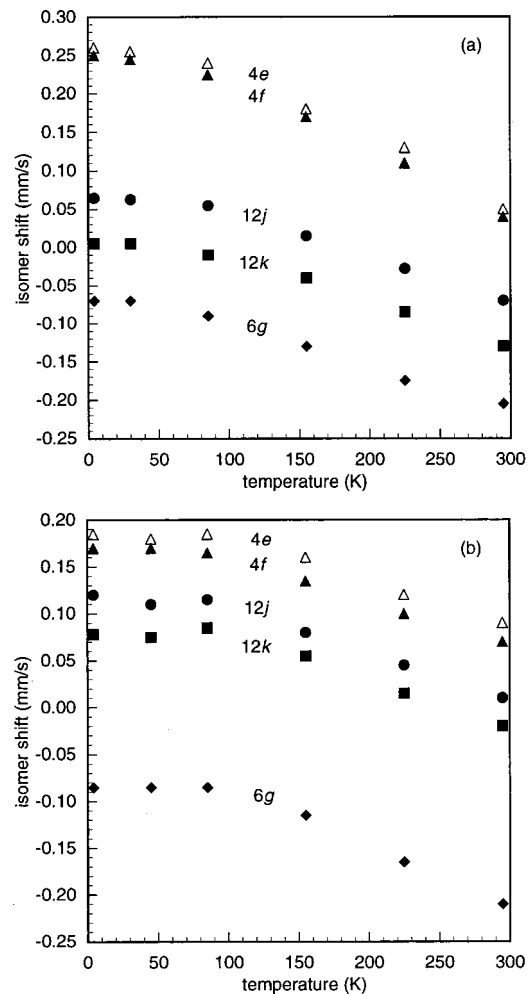


FIG. 3. The temperature dependence of the isomer shifts in (a) $\text{Ho}_2\text{Fe}_{17}$ and (b) $\text{Ho}_2\text{Fe}_{17}\text{D}_{3.8}$.

in Figs. 3(a) and 3(b), respectively. At all temperatures, the sequence of the isomer shifts, $4f > 12j > 12k > 6g$, agrees with the sequence observed^{12,13} in $\text{Dy}_2\text{Fe}_{17}$ and $\text{Er}_2\text{Fe}_{17}$. The 4e isomer shift is larger than the 4f isomer shift as was observed¹³ in $\text{Er}_2\text{Fe}_{17}$ but was not observed¹² in $\text{Dy}_2\text{Fe}_{17}$. The temperature dependence of the five isomer shifts in both compounds follows the typical second-order Doppler shift. Analysis¹⁶ of the temperature dependence of the weighted average isomer shift in $\text{Ho}_2\text{Fe}_{17}$ and $\text{Ho}_2\text{Fe}_{17}\text{D}_{3.8}$, in terms of the second-order Doppler shift, is shown in Fig. 4. The effective vibrating masses are 57 and 59 g/mol and the Mössbauer lattice temperatures are 282 and 445 K, for $\text{Ho}_2\text{Fe}_{17}$ and $\text{Ho}_2\text{Fe}_{17}\text{D}_{3.8}$, respectively. The iron effective vibrating masses and Mössbauer lattice temperatures obtained from this analysis are given in Table III together with the corresponding values for the other hexagonal $R_2\text{Fe}_{17}$ compounds and their hydride or deuteride. The accuracies of the iron effective vibrating masses and Mössbauer lattice temperatures are estimated to be 1 g/mol and 5 K, respectively. As can be seen, the effective vibrating masses and, with the exception¹⁴ of $\text{Tm}_2\text{Fe}_{17}$, which exhibits a spin-reorientation at 90 K, the Mössbauer lattice temperatures are found to be significantly larger for the hydrogen or deuterium containing compounds. Both increases indicate that the lattice of the

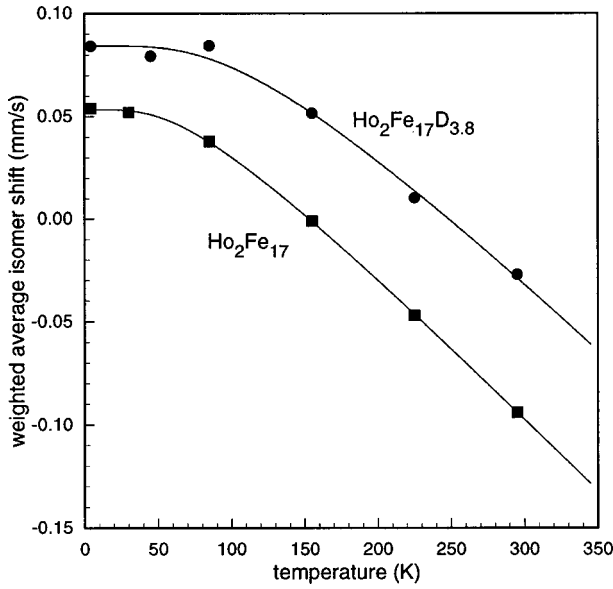


FIG. 4. The temperature dependence of the weighted average isomer shifts in $\text{Ho}_2\text{Fe}_{17}$ and $\text{Ho}_2\text{Fe}_{17}\text{D}_{3.8}$.

hydrides is more rigid and tightly bound than that of the $R_2\text{Fe}_{17}$ compounds, presumably because of the added bonding between the hydrogen or deuterium atoms and the rare-earth and iron atoms.

The temperature dependence of the site average hyperfine fields in $\text{Ho}_2\text{Fe}_{17}$ and $\text{Ho}_2\text{Fe}_{17}\text{D}_{3.8}$ is shown in Figs. 5(a) and 5(b), respectively. The 4e and 4f hyperfine fields are the largest as was observed^{12,13,17-21} in the other $R_2\text{Fe}_{17}$ compounds and the larger values agree with the larger magnetic moment of $2.55 \mu_B$ observed⁴ at 4.2 K for these two sites in both $\text{Ho}_2\text{Fe}_{17}$ and $\text{Ho}_2\text{Fe}_{17}\text{D}_{3.8}$. The hyperfine field to magnetic moment ratio is $143 \pm 5 \text{ kOe}/\mu_B$, a value which agrees perfectly with the generally accepted²² value of $145 \text{ kOe}/\mu_B$. The hyperfine field sequence, $4f > 12j \approx 6g > 12k$, in the hexagonal compounds, or $6c > 18f \approx 9g > 18h$, in the rhombohedral compounds, follows the sequence observed^{12,13,17-21} in the other $R_2\text{Fe}_{17}$ compounds and is in agreement with the increasing number of iron near neighbors, $13 > 10 = 10 > 9$. The assignment of the 12j and 12k sites is always difficult because of their equal relative areas and their similar isomer shifts. In $\text{Ho}_2\text{Fe}_{17}$ and $\text{Ho}_2\text{Fe}_{17}\text{D}_{3.8}$, their assignment is made on the basis of the quadrupole interaction of the 12j site, an interaction which is known¹⁴ to be positive and is discussed below. From the earlier neutron diffraction measurements,⁴ magnetic moments of $2.15 \mu_B$ for the 6g, 12j, and 12k iron sites in both $\text{Ho}_2\text{Fe}_{17}$ and $\text{Ho}_2\text{Fe}_{17}\text{D}_{3.8}$ have been obtained at 4.2 K. The

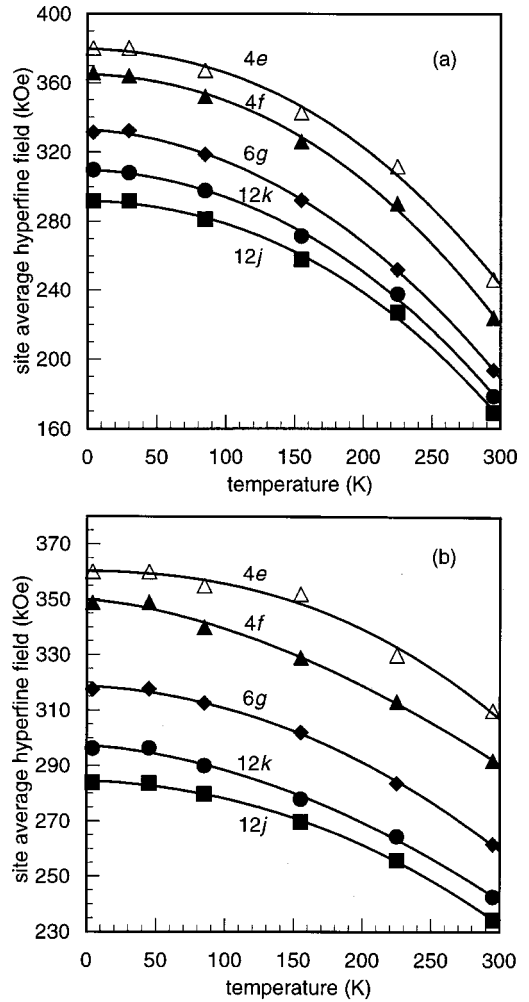


FIG. 5. The temperature dependence of the site average hyperfine fields in (a) $\text{Ho}_2\text{Fe}_{17}$ and (b) $\text{Ho}_2\text{Fe}_{17}\text{D}_{3.8}$.

Mössbauer spectral measurements are better at differentiating these three sites on the basis of their hyperfine fields than are the neutron diffraction measurements. The field to moment ratio ranges from 132 to $155 \text{ kOe}/\mu_B$, a very reasonable range of values.

The solid lines in Figs. 5(a) and 5(b) are the result of a least-squares fit²³ with the equation,

$$H = H_0 [1 - B_{3/2}(T/T_C)^{3/2} - C_{5/2}(T/T_C)^{5/2}], \quad (1)$$

where H_0 and T_C are the saturation field and the magnetic ordering temperature, respectively. The $T^{3/2}$ term in this equation has its origin²⁴ in the excitation of long-wavelength spin waves. The $B_{3/2}$ coefficients vary between 0.12 and 0.25 for the five sites in $\text{Ho}_2\text{Fe}_{17}$, and between 0.05 and 0.32 for the five sites in $\text{Ho}_2\text{Fe}_{17}\text{D}_{3.8}$. These intervals contain the values of 0.11 and 0.12 observed²⁵ for α -iron and nickel and indicate spin waves of similar wavelength. The $C_{5/2}$ coefficients are rather large at ca. 0.35 and these large values probably arise because the relatively low magnetic ordering temperatures of 335 and 500 K may limit the applicability of Eq. (1).

In all the $R_2\text{Fe}_{17}$ compounds, whether they crystallize in the rhombohedral $\text{Th}_2\text{Zn}_{17}$ -like or the hexagonal $\text{Th}_2\text{Ni}_{17}$ -like structure, the dumbbell 4f and 4e sites carry

TABLE III. Mössbauer lattice parameters for $R_2\text{Fe}_{17}\text{H}_x$.

	Parameter	Dy	Ho	Er	Tm
$R_2\text{Fe}_{17}$	m_{eff} , g/mol	57	57	57	57
	θ_M , K	306	282	265	410
$R_2\text{Fe}_{17}\text{H}_x$	x	3.8	3.8	3.6	3.2
	m_{eff} , g/mol	66	59	75	57
	θ_M , K	322	470	360	386

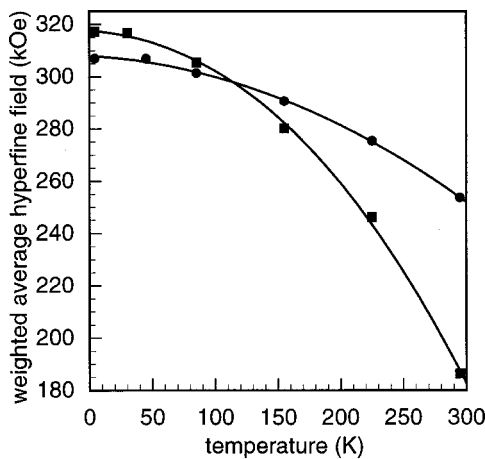


FIG. 6. The temperature dependence of the weighted average hyperfine field in $\text{Ho}_2\text{Fe}_{17}$ and $\text{Ho}_2\text{Fe}_{17}\text{D}_{3.2}$.

the largest magnetic moments^{4,26,27} of all the iron sites and also exhibit by far the largest hyperfine fields. These large magnetic moments and hyperfine fields are related to the large number of iron near neighbors of these sites, i.e., 13. The Mössbauer spectral analysis^{12–14} of the $R_2\text{Fe}_{17}$ compounds, where R is Er, Dy, Ho, and Tm, which crystallize in the hexagonal $\text{Th}_2\text{Ni}_{17}$ -like structure, reveals that the $4e$ site exhibits a larger magnetic hyperfine field and hence carries a larger magnetic moment than the $4f$ dumbbell site. Although the $4e$ and $4f$ sites have the same local symmetry and the same atomic environment, they differ slightly in the iron–iron dumbbell distance. At 280 K, the $4e$ – $4e$ distance⁴ is 2.5 Å and typically longer than the $4f$ – $4f$ distance of 2.3 Å. This longer interatomic iron–iron distance favors a ferromagnetic exchange and increases both the magnetic moment and the hyperfine field. The iron located on the $4e$ site has more available space because the percentage of substitution of a rare-earth on the $2e$ site by a dumbbell pair of irons on the $4e$ site is small in comparison with the rare-earth $2c$ replacement by the $4f$ dumbbell which is almost complete.¹²

The effect of deuterium insertion in $\text{Ho}_2\text{Fe}_{17}$ on the weighted average hyperfine field is illustrated in Fig. 6. At 4.2 K there is a small decrease in the weighted average hyperfine field upon deuterium insertion into $\text{Ho}_2\text{Fe}_{17}$ to form $\text{Ho}_2\text{Fe}_{17}\text{D}_{3.8}$. This decrease indicates that there is no increase in iron magnetic moment upon deuterium insertion, in agreement⁴ with the magnetization and neutron diffraction measurements. Because of the increase in magnetic ordering temperature upon deuterium insertion into $\text{Ho}_2\text{Fe}_{17}$ to form $\text{Ho}_2\text{Fe}_{17}\text{D}_{3.8}$, the weighted average hyperfine field in $\text{Ho}_2\text{Fe}_{17}\text{D}_{3.8}$ becomes larger above 100 K than that in $\text{Ho}_2\text{Fe}_{17}$. The solid lines in Fig. 6 are the result of a least-squares fit with Eq. (1) in which the $B_{3/2}$ coefficients are 0.19 and 0.23 and the $C_{5/2}$ coefficients are 0.35 and 0.26 for $\text{Ho}_2\text{Fe}_{17}$ and $\text{Ho}_2\text{Fe}_{17}\text{D}_{3.8}$, respectively.

The quadrupole interactions, $e^2Qq/2$, for the five inequivalent crystallographic sites do not show any significant temperature dependence. At all temperatures the asymmetry parameters were held constant and equal to the values given in Tables I and II. The quadrupole interactions obtained for $\text{Ho}_2\text{Fe}_{17}$ are very similar to those observed^{13,14} in $\text{Er}_2\text{Fe}_{17}$

and $\text{Tm}_2\text{Fe}_{17}$. The asymmetry parameter of 0.9 observed for the $12j$ site also agrees with the value of 1.0 observed¹⁴ in $\text{Tm}_2\text{Fe}_{17}$, whereas, for some unknown reason, the 0.0 asymmetry parameter observed for the $12k$ site disagrees with the 1.0 value observed¹⁴ in $\text{Tm}_2\text{Fe}_{17}$. However, in $\text{Ho}_2\text{Fe}_{17}$ fits with the asymmetry parameter for the $12k$ site set equal to one are substantially poorer. The θ angles observed for the magnetically inequivalent $12j$ and $12k$ sites differ by 60 deg, a difference which is compatible with the hexagonal symmetry of these sites.

In going from $\text{Ho}_2\text{Fe}_{17}$ to $\text{Ho}_2\text{Fe}_{17}\text{D}_{3.8}$, there is no significant variation of the quadrupole interactions for the five iron sites, as is indicated by the values given in Tables I and II. This invariance is certainly expected for the $4e$, $4f$, and $6g$ sites whose environments are unchanged by the insertion of deuterium into the lattice. In contrast, some variation could have been expected for the quadrupole interactions of the $12j$ and $12k$ sites, the sites which have at least one deuterium near neighbor in $\text{Ho}_2\text{Fe}_{17}\text{D}_{3.8}$. However, the addition of only a unit charge in the neighborhood of the iron site may not significantly alter the quadrupole interaction at this site. In going from $\text{Ho}_2\text{Fe}_{17}$ to $\text{Ho}_2\text{Fe}_{17}\text{D}_{3.8}$ the asymmetry parameters of the $4e$, $4f$, $6g$, and $12j$ sites are unchanged, whereas the asymmetry parameter of the $12k$ site increases from 0.0 to 0.8. This increase may be related to the additional $12i$ hydrogen near neighbor of the $12k$ iron site. In going from $\text{Ho}_2\text{Fe}_{17}$ to $\text{Ho}_2\text{Fe}_{17}\text{D}_{3.8}$ there are at most small changes in the θ angles. For $\text{Ho}_2\text{Fe}_{17}\text{D}_{3.8}$ slightly better fits were obtained by introducing a temperature dependence of the θ angles for the $6g$ and $12j$ sites. This temperature dependence may indicate that the principal axis of the electric field gradient is slightly reorienting its position relative to the direction of the hyperfine field because of the lattice expansion with increasing temperature.

The filling by deuterium of the disordered hexagonal $\text{Ho}_2\text{Fe}_{17}$ structure terminates at almost four deuterium atoms per formula unit. In contrast to the $R_2\text{Fe}_{17}$ compounds, which crystallize in the rhombohedral $\text{Th}_2\text{Zn}_{17}$ -like structure and can accommodate up to three hydrogen or deuterium atoms in the octahedral $9e$ sites, less than three deuterium atoms occupy the octahedral $6h$ sites in $\text{Ho}_2\text{Fe}_{17}$. It seems that the presence of the excess iron found on the $4e$ site hampers the complete filling by deuterium of the neighboring interstitial octahedral $6h$ sites. Because deuterium fills approximately one of the six tetrahedral sites, the six $12i$ sites that form a hexagon, dynamic motion of the deuterium between the six sites is expected. Indeed, there is no evidence in the Mössbauer spectra for any slowing down of the dynamic motion of the deuterium on the Mössbauer-effect timescale. In contrast, in rhombohedral $\text{Pr}_2\text{Fe}_{17}\text{D}_5$, in which two deuterium atoms occupy two of the six $18g$ sites, the dynamic motion is blocked¹⁸ below 85 K.

The dependence of the 85 K weighted average isomer shift in $R_2\text{Fe}_{17}$, $R_2\text{Fe}_{17}\text{H}_x$, and $R_2\text{Fe}_{17}\text{N}_3$, as a function of the rare-earth atom is shown in Fig. 7. From Nd to Tm, there is a general decrease in the weighted average isomer shift of $R_2\text{Fe}_{17}$ and $R_2\text{Fe}_{17}\text{H}_x$ with increasing rare-earth atomic number, a decrease which parallels the lanthanide contraction. As the unit-cell volume decreases, the s -electron density at the

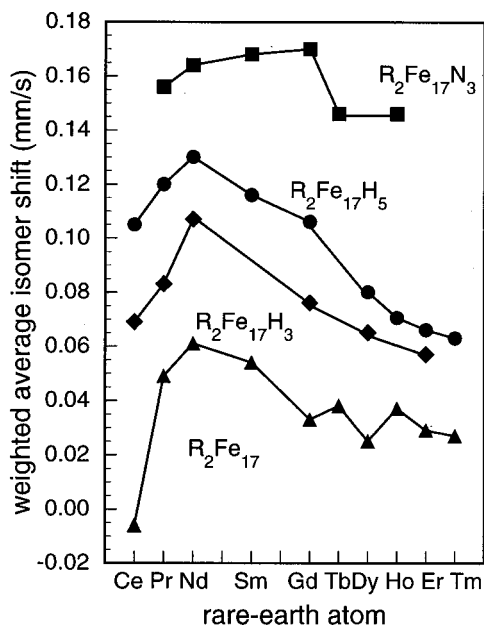


FIG. 7. The 85 K weighted average isomer shift in R_2Fe_{17} , $R_2Fe_{17}H_x$, and $R_2Fe_{17}N_3$, as a function of the rare-earth atom. In these plots for $R_2Fe_{17}H_5$ data for samples with the maximum amount of hydrogen have been used if compounds with $x=5$ could not be obtained.

iron nucleus increases and, hence, the isomer shift decreases. For all rare-earth atoms, the isomer shift increases with insertion of three hydrogen atoms, increases further with insertion of two more hydrogen atoms, and increases even further with the insertion of three nitrogen atoms. These subsequent increases parallel the concomitant increases of the unit-cell volume.

The insertion of deuterium into α -iron to form ϵ - $FeH_{0.8}$ is known²⁸ to increase the isomer shift by approximately 0.5 mm/s, a very large increase that results from the close to one to one hydrogen to iron ratio in ϵ - $FeH_{0.8}$. The analogous increase between Ho_2Fe_{17} and $Ho_2Fe_{17}D_{3.8}$ is about 0.05 mm/s at low temperature. This significant but relatively small increase can be understood in terms of the smaller deuterium to iron ratio in $Ho_2Fe_{17}D_{3.8}$. On the basis of the hydrogen to iron ratio, an increase of 0.11 mm/s would be expected. Similar changes in the isomer shift are obtained for other R_2Fe_{17} compounds where R is Sm, Nd, Gd, Dy, and Er. In Ce_2Fe_{17} the observed increase in the isomer shift upon hydrogen or deuterium insertion is much larger at ca. 0.10 mm/s, but it is worth noting that in this compound, the insertion of hydrogen induces a larger expansion⁴ of the unit cell and a change from helimagnetic to ferromagnetic ordering.¹⁷

The dependence of the 85 K weighted average hyperfine field in R_2Fe_{17} , $R_2Fe_{17}H_x$, and $R_2Fe_{17}N_3$, as a function of the rare-earth atom is shown in Fig. 8. In this figure, for easy comparison purposes, the very small value of 198 kOe for Ce_2Fe_{17} , which has a spiral magnetic structure is omitted and the 100 K value is used for Tm_2Fe_{17} , because at 85 K this compound shows¹⁴ a mixture of axial and basal magnetic anisotropies. $Pr_2Fe_{17}H_3$, $Pr_2Fe_{17}H_5$, and $Sm_2Fe_{17}N_3$, which all exhibit a preferential axial orientation of the magnetic moments, show large values for their hyperfine fields in

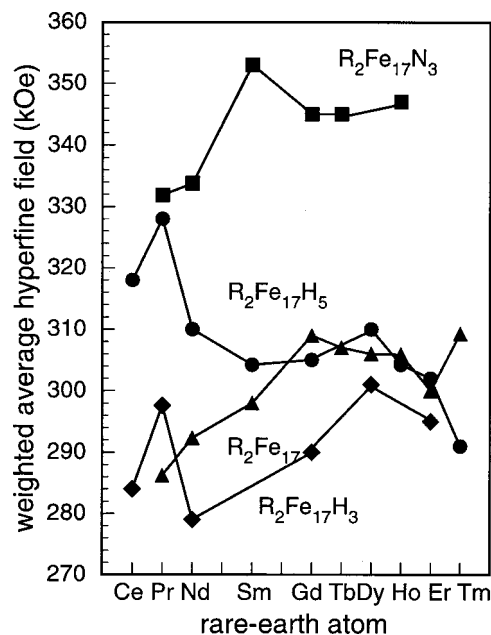


FIG. 8. The 85 K weighted average hyperfine field in R_2Fe_{17} , $R_2Fe_{17}H_x$, and $R_2Fe_{17}N_3$, as a function of the rare-earth atom. In these plots for $R_2Fe_{17}H_5$ data for samples with the maximum amount of hydrogen have been used if compounds with $x=5$ could not be obtained.

their respective series of compounds. The increased hyperfine field observed in these compounds can be understood¹⁴ in terms of a decreased orbital contribution to the hyperfine field resulting from the axial orientation of the iron magnetic moments. For the rare-earth atoms heavier than Pr, the weighted average hyperfine field in the $R_2Fe_{17}H_3$ compounds are smaller than in the R_2Fe_{17} compounds. This decrease in hyperfine field agrees with the decrease⁸ in magnetization upon insertion of three hydrogen atoms into the R_2Fe_{17} compounds. For the rare-earth atoms lighter and heavier than Gd, the weighted average hyperfine field in the $R_2Fe_{17}H_5$ compounds are larger and smaller, respectively, than in the R_2Fe_{17} compounds. For all rare-earth atoms, the weighted average hyperfine field in the $R_2Fe_{17}N_3$ compounds are larger than in the R_2Fe_{17} and $R_2Fe_{17}H_x$ compounds.

ACKNOWLEDGMENTS

The authors thank Z. Lin for help in obtaining the Mössbauer spectral data. G.J.L. thanks the US National Science Foundation for Grants Nos. DMR95-21739 and INT-9815138, and the "Fonds National de la Recherche Scientifique," Brussels, Belgium, for support during a sabbatical leave during the 2000–2001 academic year. O.I. thanks the "Center National de la Recherche Scientifique, France" for grant action initiative No. 7418.

¹K. H. J. Buschow, *J. Less-Common Met.* **11**, 204 (1966).

²D. Givord and R. Lemaire, *C. R. Acad. Sci. (Paris)* **274**, 1166 (1966).

³A. N. Christensen and R. G. Hazell, *Acta Chem. Scand., Ser. A* **34**, 455 (1980).

⁴O. Isnard, S. Miraglia, J. L. Soubeyrou, D. Fruchart, and A. Stergiou, *J. Less-Common Met.* **162**, 273 (1990).

⁵D. Fruchart, M. Bacmann, P. de Rango, O. Isnard, S. Liesert, S. Miraglia,

- S. Obbade, J. L. Soubeyroux, E. Tomey, and P. Wolfers, *J. Alloys Compd.* **253–254**, 121 (1997).
- ⁶O. Isnard, S. Miraglia, D. Fruchart, E. Akiba, and K. Nomura, *J. Alloys Compd.* **257**, 150 (1997).
- ⁷O. Isnard, J. L. Soubeyroux, S. Miraglia, D. Fruchart, L. M. Garcia, and J. Bartolomé, *Physica B* **180**, 629 (1992).
- ⁸O. Isnard, S. Miraglia, J. L. Soubeyroux, D. Fruchart, and P. L'Héritier, *J. Magn. Magn. Mater.* **137**, 151 (1994).
- ⁹G. Westlake, *J. Less-Common Met.* **90**, 251 (1983).
- ¹⁰D. Givord, Ph.D. Thesis, University of Grenoble (1973).
- ¹¹D. Givord and R. Lemaire, *IEEE Trans. Magn.* **10**, 109 (1974).
- ¹²O. Isnard, D. Hautot, G. J. Long, and F. Grandjean, *J. Appl. Phys.* **88**, 2750 (2000).
- ¹³F. Grandjean, O. Isnard, D. Hautot, and G. J. Long, *Phys. Rev. B* **63**, 014406 (2001).
- ¹⁴F. Grandjean, O. Isnard, and G. J. Long, *Phys. Rev. B* (submitted).
- ¹⁵J. Bartolomé, in *Interstitial Intermetallic Alloys*, edited by G. J. Long, F. Grandjean, and K. H. J. Buschow (Kluwer, Dordrecht, 1994), p. 541.
- ¹⁶G. J. Long, D. Hautot, F. Grandjean, D. T. Morelli, and G. P. Meisner, *Phys. Rev. B* **60**, 7410 (1999).
- ¹⁷D. Hautot, G. J. Long, F. Grandjean, and O. Isnard, *Phys. Rev. B* **62**, 11 731 (2000).
- ¹⁸D. Hautot, G. J. Long, F. Grandjean, O. Isnard, and S. Miraglia, *J. Appl. Phys.* **86**, 2200 (1999).
- ¹⁹F. Grandjean, D. Hautot, G. J. Long, O. Isnard, S. Miraglia, and D. Fruchart, *J. Appl. Phys.* **85**, 4654 (1999).
- ²⁰G. J. Long, O. A. Pringle, F. Grandjean, and K. H. J. Buschow, *J. Appl. Phys.* **72**, 4845 (1992).
- ²¹G. J. Long, S. Mishra, O. A. Pringle, F. Grandjean, and K. H. J. Buschow, *J. Appl. Phys.* **75**, 5994 (1994).
- ²²R. Coehoorn, *J. Magn. Magn. Mater.* **99**, 55 (1991).
- ²³H. N. Ok, K. S. Baek, and C. S. Kim, *Phys. Rev. B* **24**, 6600 (1981).
- ²⁴C. Herring and C. Kittel, *Phys. Rev.* **81**, 869 (1951).
- ²⁵B. E. Argyle, S. H. Charap, and E. W. Pugh, *Phys. Rev.* **132**, 2051 (1963).
- ²⁶P. C. M. Gubbens, Ph.D. Thesis, Delft University (1977).
- ²⁷G. J. Long, O. A. Pringle, F. Grandjean, W. B. Yelon, and K. H. J. Buschow, *J. Appl. Phys.* **74**, 504 (1993).
- ²⁸R. Wordel, F. E. Wagner, V. E. Antonov, E. G. Ponyatovskii, A. Permogorov, A. Plachinda, and E. F. Makarov, *Hyperfine Interact.* **28**, 1005 (1986).